Composites Science and Technology 144 (2017) 1–10

Contents lists available at ScienceDirect

Composites Science and Technology

journal homepage: http://www.elsevier.com/locate/compscitech

Roles of carbon nanotube and $BaTiO_3$ nanofiber in the electrical, dielectric and piezoelectric properties of flexible nanocomposite generators

Jing Yan, Young Gyu Jeong*

Department of Advanced Organic Materials and Textile System Engineering, Chungnam National University, Daejeon, 34134, Republic of Korea

ARTICLE INFO

Article history:
Received 30 July 2016
Received in revised form
10 December 2016
Accepted 14 March 2017
Available online 15 March 2017

Keywords:
$BaTiO_3$ nanofiber
Multi-walled carbon nanotube
Nanocomposite generator
Piezoelectricity
Polydimethylsiloxane

ABSTRACT

We report the electrical, dielectric and piezoelectric properties of flexible PDMS-based nanocomposite generators, which are tunable by different contents of multi-walled carbon nanotube (MWCNT, 0.0–5.0 wt%) and $BaTiO_3$ nanofiber (10–50 wt%). The $BaTiO_3$ nanofiber with tetragonal structure was manufactured by an electrospinning and following calcination process. For the first series of nanocomposite generators with 30 wt% $BaTiO_3$ nanofiber and 0.0–5.0 wt% MWCNT, both electrical and dielectric properties were dramatically enhanced at a critical MWCNT content of 0.47 wt% owing to the formation of percolating networks of MWCNT in the presence of $BaTiO_3$ nanofibers, as verified by SEM analysis. Accordingly, the nanocomposite generator with 30 wt% $BaTiO_3$ and 5.0 wt% MWCNT achieved the highest conductivity of 0.12 S/cm and dielectric constant of 4474 at 1 kHz, whereas the nanocomposite generator with 30 wt% $BaTiO_3$ and 2.0 wt% MWCNT attained the best piezoelectric performance by harvesting average output voltage of ~3.00 V, current of ~0.82 μA, and power of ~0.14 μW. In cases of the second series of nanocomposite generators with 2.0 wt% MWCNT and 10–50 wt% $BaTiO_3$ nanofiber, the electrical conductivity and dielectric constant increased with the increment of $BaTiO_3$ content up to 40 wt%. Overall, the nanocomposite generator with 2.0 wt% MWCNT and 40 wt% $BaTiO_3$ nanofiber generated the highest average output voltage of ~3.73 V, current of ~1.37 μA, and power of ~0.33 μW, which was feasible to light up commercial LEDs and to charge a capacitor after rectification, revealing the potentiality in powering self-sufficient nanodevices and wireless electronics.

© 2017 Elsevier Ltd. All rights reserved.

1. Introduction

Piezoelectric nanocomposite generators (PNGs) have gained tremendous attention from both industry and academia because they can harvest energy from mechanical actions to power electric devices instantly, which thus alleviates the energy crisis and environmental problems [1,2]. Nowadays, the widely known piezoelectric materials include lead zirconate titanate (PZT), barium titanate ($BaTiO_3$), zinc oxide (ZnO), zinc sulfide (ZnS), poly(vinylidene fluoride) (PVDF), etc. Among the piezoelectric materials, $BaTiO_3$ with high piezoelectric coefficient (149 pC/N) and dielectric constant (100–11000) is one of the most promising lead-free perovskite-structured materials [1,3–10].

To improve the piezoelectric property of PNGs, intensive efforts have been made by introducing nanofillers. Carbon nanotubes (CNTs) with excellent electrical and physical properties have been used abundantly as reinforcing fillers in composite materials to evaluate the effect of its content on various properties for a number of advanced applications [11,12]. The incorporation of CNTs in PNGs also plays an important role in the piezoelectric property for different reasons. Park et al. reported that a nanocomposite including 12 wt% $BaTiO_3$ nanoparticle and 1 wt% multi-walled carbon nanotube (MWCNT) achieved an increase of output voltage from 0.17 to 3.2 V under bending deformation due to better distribution of nanoparticles and stress enhancement by adding MWCNT [2]. Sun et al. reported that a nanocomposite containing 12 wt% ZnO nanoparticles and 1 wt% MWCNT exhibited significantly enhanced output voltage of 7.5 V owing to the presence of MWCNT serving as “nano-electrical bridge” between ZnO nanoparticles, compared with a nanocomposite with only ZnO nanoparticle (0.8 V) [13]. Ahn et al. and Hao et al. have investigated the

* Corresponding author.
E-mail address: ygjeong@cnu.ac.kr (Y.G. Jeong).

http://dx.doi.org/10.1016/j.compscitech.2017.03.015
0266-3538/© 2017 Elsevier Ltd. All rights reserved.

effect of the MWCNT content on the piezoelectric properties of PVDF/MWCNT nanocomposites manufactured by an electrospinning process and have found that a dramatic increase in the β-phase crystal formation with higher MWCNT loadings due to the intense stretching of PVDF during the electrospinning [14,15]. It is thus considered that MWCNT serves as a nucleating agent for developing β-phase PVDF crystals during the electrospinning process as well as an electrical bridge among the piezoelectric PVDF crystals in the nanocomposites.

The amount of the piezoelectric materials is also an important factor influencing the piezoelectric performance of PNGs. Mahadeva et al. fabricated hybrid piezoelectric papers by attaching $BaTiO_3$ nanoparticles to the positively charged wood cellulose fibers via a strong electrostatic interaction prior to the process of making paper sheets [16]. Piezoelectric response of the hybrid paper was found to increase significantly with increment of $BaTiO_3$ loading. The effective piezoelectric coefficient, d_{33}, increased from 1.02 pC/N for the paper with 11 wt% $BaTiO_3$ to 4.8 pC/N for the paper with the highest nanoparticle loading of 48 wt% $BaTiO_3$. In case of P(VDF-TrFE)/$BaTiO_3$ composites, d_{33} also increased with the increment of the $BaTiO_3$ content, reaching a highest value of 32 pC/N at the $BaTiO_3$ content of 60 wt% [17].

In this study, the roles of $BaTiO_3$ nanofiber and MWCNT in the electrical, dielectric and piezoelectric properties of flexible nanocomposite generators were investigated. The $BaTiO_3$ nanofiber with tetragonal structure was manufactured via an electrospinning and following calcination process. Because $BaTiO_3$ nanofibers are brittle and they cannot be used solely, polydimethylsiloxane (PDMS) as a highly flexible silicone-based elastomer was adopted as the nanocomposite matrix. For the purpose, PDMS-based flexible PNGs with different contents of MWCNT (0.0–5.0 wt%) and $BaTiO_3$ nanofiber (10–50 wt%) were fabricated. The electrical, dielectric and piezoelectric properties of the flexible PNGs were then investigated systematically by taking into account the roles and contents of MWCNT and $BaTiO_3$ nanofiber in the PNGs. The harvested piezoelectric energy was also evaluated to light up commercial light-emitting diodes (LEDs) and to charge a capacitor after rectification.

2. Experimental

2.1. Preparation of $BaTiO_3$ nanofiber and piezoelectric nanocomposite generators (PNGs)

$BaTiO_3$ nanofibers were prepared by electrospinning a sol-gel precursor and following calcination process as described in literature [6,18]. Barium acetate (2.55 g, Sigma-Aldrich Com.), titanium butoxide (3.4 g, Sigma-Aldrich Com.), and 2,4-pentanedione (2.0 g, Samchun Pure Chemical Com.) were dissolved in acetic acid (6 ml, Samchun Pure Chemical Com.) by magnetic stirring for 24 h to form a homogeneous sol-gel precursor. Poly(vinyl pyrrolidone) (PVP, 1.0 g, Sigma-Aldrich Com.) was added into the solution to control the viscosity and stirred magnetically for 12 h. To fabricate precursor nanofibers, the sol-gel precursor solution was electrospun at a condition of voltage of 15 kV, tip-to-collector distance of 18 cm, extrusion rate of 1 ml/h, and collector rotating speed of 800 RPM. The fabricated precursor nanofibers were calcined to form $BaTiO_3$ ceramic nanofibers by increasing temperature stepwise to 1000 °C and finally holding at 1000 °C for 6 h.

To manufacture flexible PNGs with various $BaTiO_3$ nanofiber and MWCNT contents, predetermined amounts of MWCNT (CM-95, diameter of 10–15 nm, length of 10–20 μm, Hanwha Chemical) (0.0–5.0 wt%) and $BaTiO_3$ nanofiber (10–50 wt%) were dispersed ultrasonically in ethyl acetate for 1 h using a bath-type ultrasonicator (50–60 Hz). After adding PDMS (Sylgard 184 Silicone Elastomer Kit, Dow Corning) into ethyl acetate solutions, another ultrasonication was applied for 1 h. Subsequently, a curing agent (weight ratio of 1:10 to base paste) was added into the solutions, which were then poured into glass petri-dishes. After evaporating the solvent totally, composite pastes were casted on Scotch tape-coated glass substrates to be ~250 μm thick by a doctor-blade. Finally, the composites were cured on a hot plate at 100 °C for 12 h. The fabricated specimens were named as PDMS/$BaTiO_3$(X)/MWCNT(Y), where X and Y denote the relative contents of $BaTiO_3$ nanofiber and MWCNT in the PNGs by wt%, respectively, as summarized in Table 1. For an electric poling process, the PNGs were sandwiched by Aluminum foil-attached cover slides and poled under an electric field of 5 kV/mm for 12 h in a bath containing silicone oil (KF-96, Shin-Etsu Silicone Korea Co., Ltd) at ambient temperature. Then, electrically poled specimens were rinsed with ethanol to remove the silicone oil and Aluminum foil as an electrode was attached on the top and bottom sides of the PNGs.

2.2. Characterization

The morphological features of $BaTiO_3$ nanofiber and flexible PNGs were characterized by using a cold type field emission scanning electron microscope (SEM, S-4800, Hitachi). To obtain the SEM images, the fracture surfaces of the PNGs were coated with osmium conductive metal. The crystal structure of $BaTiO_3$ nanofiber was identified by a high performance X-ray diffractometer using Cu-Kα radiation (D/MAX-2200 Ultima/PC, Rigaku). The electrical current of the PNGs was measured as a function of applied voltage by using an electrometer (2400, Keithley Instruments). The frequency-dependent electrical and dielectric properties of the PNGs were measured by using a precision LCR meter (4980A, Agilent). The piezoelectric performance of the PNGs under a periodically applied finger pressure of 2 kPa was evaluated with aid of 7½-digit graphical sampling multimeter (Keithley Instruments).

3. Results and discussion

3.1. Structures of $BaTiO_3$ nanofiber

$BaTiO_3$ nanofibers were fabricated by an electrospinning of the precursor solution and following calcination process [19]. The SEM image and XRD pattern of Fig. 1(a)-(b) reveal that $BaTiO_3$ nanofibers with a tetragonal crystal phase, which are evident by the appearance of (002) and (200) reflections separated at $2\theta = \sim 45^\circ$, are well manufactured by the electrospinning and calcination process. To apply $BaTiO_3$ nanofibers into PDMS for manufacturing the flexible PNGs, an ultrasonication technique was adopted to disperse $BaTiO_3$ nanofibers in ethyl acetate initially, in which case $BaTiO_3$ nanofibers were broken randomly into short nanofibers as shown in the SEM image of Fig. 1(c). It was found that $BaTiO_3$ nanofibers have an average length of ~33.7 μm and an average diameter of ~354.1 nm, as represented in Fig. 1(d) and (e), respectively.

3.2. Role of MWCNT on structures and properties of PNGs

The cross-sectional SEM images (× 1000) of PNGs with 30 wt% $BaTiO_3$ nanofiber and different MWCNT contents of 0.0–5.0 wt% are shown in Fig. 2. Some pores detected in the images were formed by the pulling-out of $BaTiO_3$ nanofibers from the PDMS matrix, because the PNGs were fractured for SEM test. From the magnified cross-sectional SEM images (× 5000) of the PNGs. MWCNTs are found to be dispersed uniformly and randomly in the PDMS matrix

Table 1
AC conductivity, dielectric constant, and piezoelectric performance of PDMS-based nanocomposite generators with different contents of $BaTiO_3$ nanofiber (10–50 wt%) and MWCNT (0.0–5.0 wt%).

Nanogenerators	PDMS content (wt%)	$BaTiO_3$ nanofiber content (wt%)	MWCNT content (wt%)	AC conductivity at 1 kHz (S/cm)	Dielectric constant at 1 kHz	Output voltage (V)	Output current (μA)	Output power (μW)
PDMS/$BaTiO_3$(30)/MWCNT(0.0)	70	30	0.0	2.93×10^{-9}	5.67	0.58 ± 0.028	0.058 ± 0.0015	0.0061 ± 0.0032
PDMS/$BaTiO_3$(30)/MWCNT(1.0)			1.0	1.11×10^{-3}	2069.4	0.94 ± 0.03	0.15 ± 0.002	0.0188 ± 0.0011
PDMS/$BaTiO_3$(30)/MWCNT(2.0)			2.0	9.27×10^{-2}	2455.4	3.00 ± 0.12	0.82 ± 0.02	0.1401 ± 0.0278
PDMS/$BaTiO_3$(30)/MWCNT(3.0)			3.0	4.33×10^{-2}	3817.9	1.30 ± 0.04	0.54 ± 0.03	0.0266 ± 0.0051
PDMS/$BaTiO_3$(30)/MWCNT(5.0)			5.0	1.18×10^{-1}	4744.8	0.27 ± 0.02	0.08 ± 0.003	0.0024 ± 0.0002
PDMS/$BaTiO_3$(10)/MWCNT(2.0)	90	10	2.0	1.55×10^{-4}	1462.5	0.69 ± 0.07	0.21 ± 0.02	0.0205 ± 0.0017
PDMS/$BaTiO_3$(20)/MWCNT(2.0)	80	20		4.12×10^{-3}	1728.4	2.04 ± 0.20	0.75 ± 0.07	0.1043 ± 0.0210
PDMS/$BaTiO_3$(40)/MWCNT(2.0)	60	40		4.76×10^{-2}	3329.9	3.73 ± 0.11	1.37 ± 0.24	0.3293 ± 0.0566
PDMS/$BaTiO_3$(50)/MWCNT(2.0)	50	50		1.75×10^{-1}	3635.0	0.91 ± 0.06	0.10 ± 0.01	0.0193 ± 0.0044

without any apparent agglomeration, and more MWCNTs can be identified in the PNGs with higher MWCNT contents. $BaTiO_3$ nanofibers are also dispersed homogeneously in the PDMS matrix. It is thus reasonable to mention that the manufacturing procedure used in this study is effective and facile to fabricate the flexible PNGs.

The electrical, dielectric and piezoelectric properties of the PNGs with constant 30 wt% $BaTiO_3$ nanofiber were investigated as a function of the MWCNT content of 0.0–5.0 wt%. The current-voltage (*I-V*) curves of all the PNGs with different MWCNT contents are represented in Fig. 3(a) which depicts positive changes with boosted applied voltage. The applied voltage of PNGs with

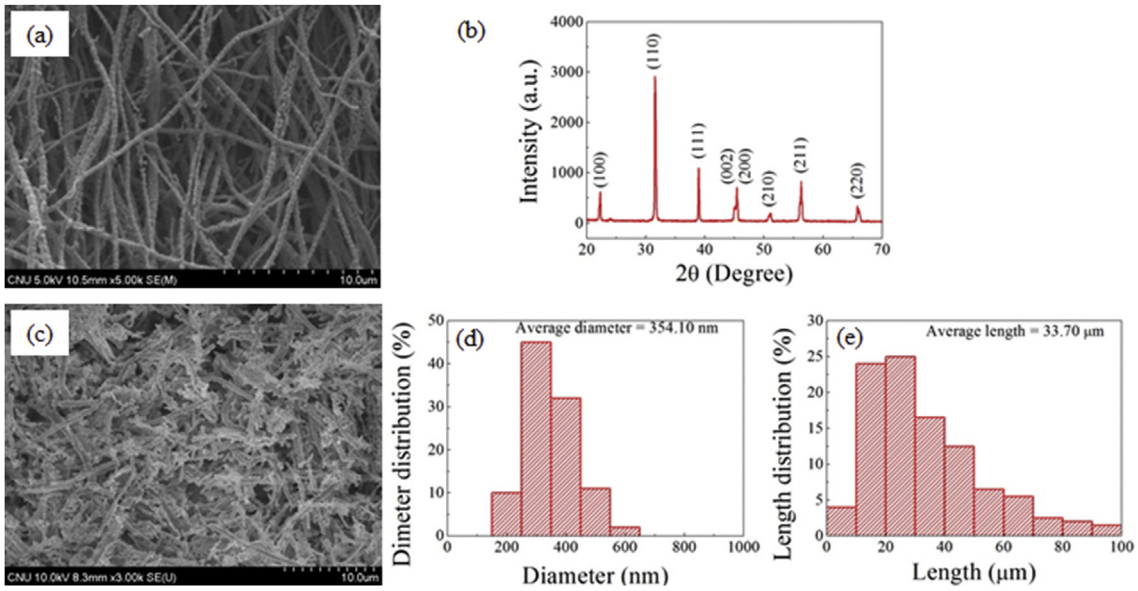

Fig. 1. (a) SEM image and (b) XRD spectrum of $BaTiO_3$ nanofibers manufactured by an electrospinning and following calcination; (c) SEM image, (d) diameter distribution, and (e) length distribution of $BaTiO_3$ nanofibers after ultrasonication.

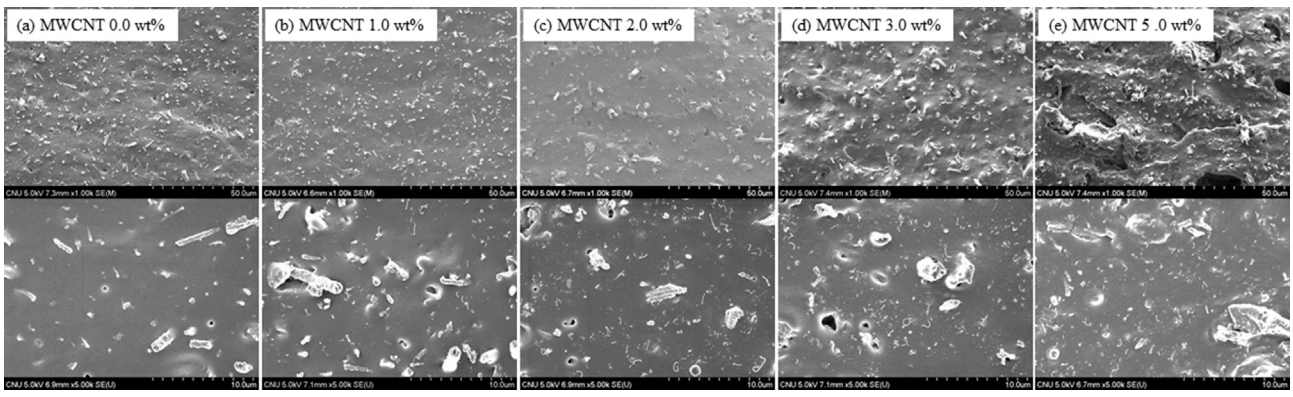

Fig. 2. Cross-sectional SEM images of PNGs with 30 wt% $BaTiO_3$ nanofiber and different MWCNT contents (0.0–5.0 wt%).

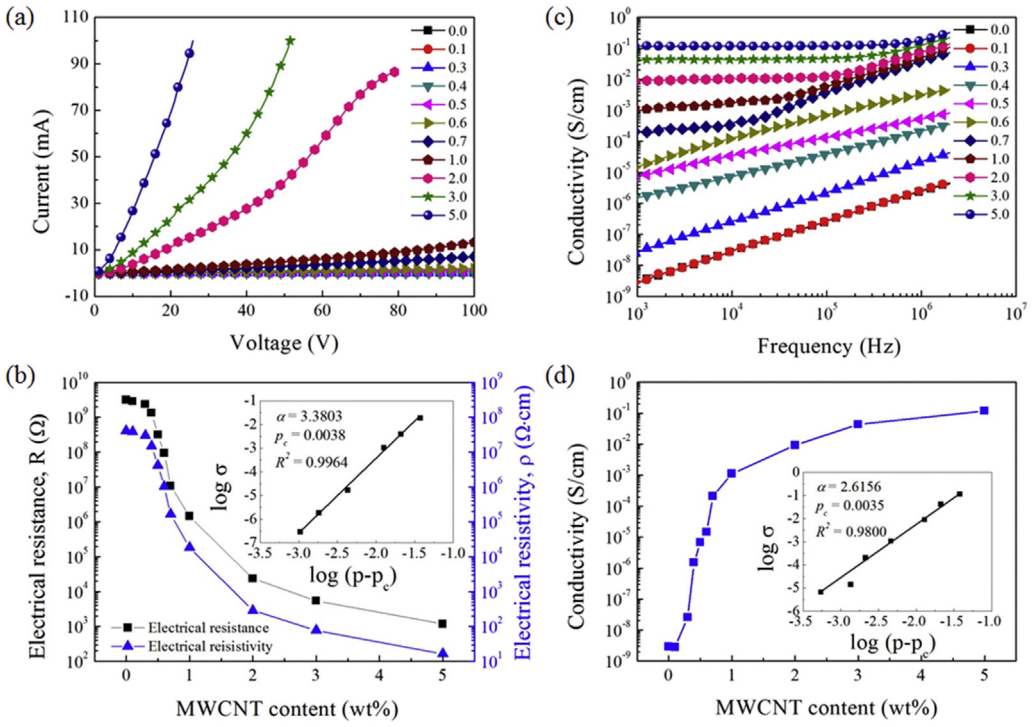

Fig. 3. (a) Current-voltage curves and (b) electrical resistance and resistivity of PNGs with 30 wt% $BaTiO_3$ nanofiber and different MWCNT contents (0.0–5.0 wt%); (c) AC conductivity-frequency curves and (d) AC conductivity at 1 kHz of PNGs with 30 wt% $BaTiO_3$ nanofiber and different MWCNT contents (0.0–5.0 wt%). Insets in (b) and (d) are log σ *vs.* log (p-p_c) plot from the power law relation with the experimental electrical conductivity data.

2.0–5.0 wt% MWCNT was terminated before 100 V due to the thermal degradation of the PNGs under over-high temperature caused by the electric heating effect [20]. The electrical resistance R of the PNGs was evaluated at an applied voltage of 1 V. The electrical resistivity ρ could then be calculated by using the equation $R = \rho(L/A)$, where L is the sample length between electrodes (1 cm) and A is the cross-sectional area of a specimen. The resulting electrical resistance and resistivity of the PNGs were plotted as a function of the MWCNT content, as shown in Fig. 3(b). It is found that electrical resistivity decreased dramatically from ~10^7 Ω cm for PDMS/$BaTiO_3$(30)/MWCNT(0.0) to ~10^1 Ω cm for PDMS/$BaTiO_3$(30)/MWCNT(5.0) by displaying a typical percolation behavior. A critical volume fraction p_c at the electrical percolation can be determined by the power law relation $\sigma \sim (p\text{-}p_c)^{\alpha}$ where σ is the electrical conductivity (the inverse of electrical resistivity), p is the MWCNT volume fraction, and α is the critical exponent. The calculated p_c was ~0.38 vol% (~0.47 wt%), which is a considerably low value due to the effective dispersion of MWCNT in the PNGs. The logσ *vs.* log(p-p_c) plot of the power law relation with the experimental electrical conductivity data was shown in the inset of Fig. 3(b). The critical exponent 3.3803 is higher than the theoretical value of 1.94 for an ideal system with 3-dimensional (3-D) random dispersion of spherical particles, which may be associated with the random orientation of anisotropic 1-D MWCNTs in the presence of 30 wt% $BaTiO_3$ nanofiber [20]. The AC conductivity of the PNGs was measured in the frequency from 1 kHz to 2 MHz, as represented in Fig. 3(c). The AC conductivity of the PNGs with low MWCNT contents (0.1–0.6 wt%) increased continuously with the increment of the frequency. For the PNGs with higher MWCNT contents (0.7–5.0 wt%), the AC conductivity remained unchanged at low frequency range due to the percolation formation of MWCNTs, while above critical frequencies they increased again with the frequency. The constant AC conductivity extended to higher frequency ranges for the PNGs with higher MWCNT content, which phenomenon is known as “universal dynamic response” [21,22]. Based on the change of AC conductivity of the PNGs at 1 kHz with the MWCNT content as displayed in Fig. 3(d), the percolation threshold of MWCNT could be estimated to be p_c of ~0.35 vol% (~0.43 wt%), which is quite consistent with the value of ~0.38 vol% in Fig. 3(b).

The frequency-dependent dielectric constant changes of the PNGs with different MWCNT contents are showed in Fig. 4(a). It demonstrates that the frequency dependency of the dielectric constants was quite weak for the PNGs with MWCNTs below 0.4 wt % or above 1.0 wt%, while for the PNGs with MWCNTs of 0.4–1.0 wt %, the dielectric constant decreased noticeably with the increment of the frequency. When the dielectric constant at 1 kHz was plotted as a function of the MWCNT content in the PNGs (Fig. 4(b)), it changed drastically at the MWCNT content range of 0.4–1.0 wt%, which is close to a critical concentration evaluated by the percolation theory. The high dielectric constant was achieved for the PNGs with high MWCNT loadings, which is explained by the microcapacitor principle that has been accountable to other composites with MWCNT or graphene nanofillers [23–25]. For the PNGs in this study, the conductive MWCNT fillers distributed in the PDMS matrix can form a lot of microcapacitors whose number increases with increasing the amount of MWCNT fillers. The isolation distances among MWCNT fillers in the PNGs decrease with increasing the MWCNT content so that the average capacitance of the microcapacitors increases. As a result, the dielectric constants of the PNGs with higher MWCNT contents are enhanced remarkably. The frequency-dependent loss tangent and its variation with MWCNT loading are illustrated in Fig. 4(c) and (d), respectively, which demonstrate a strong decline of loss tangent with the

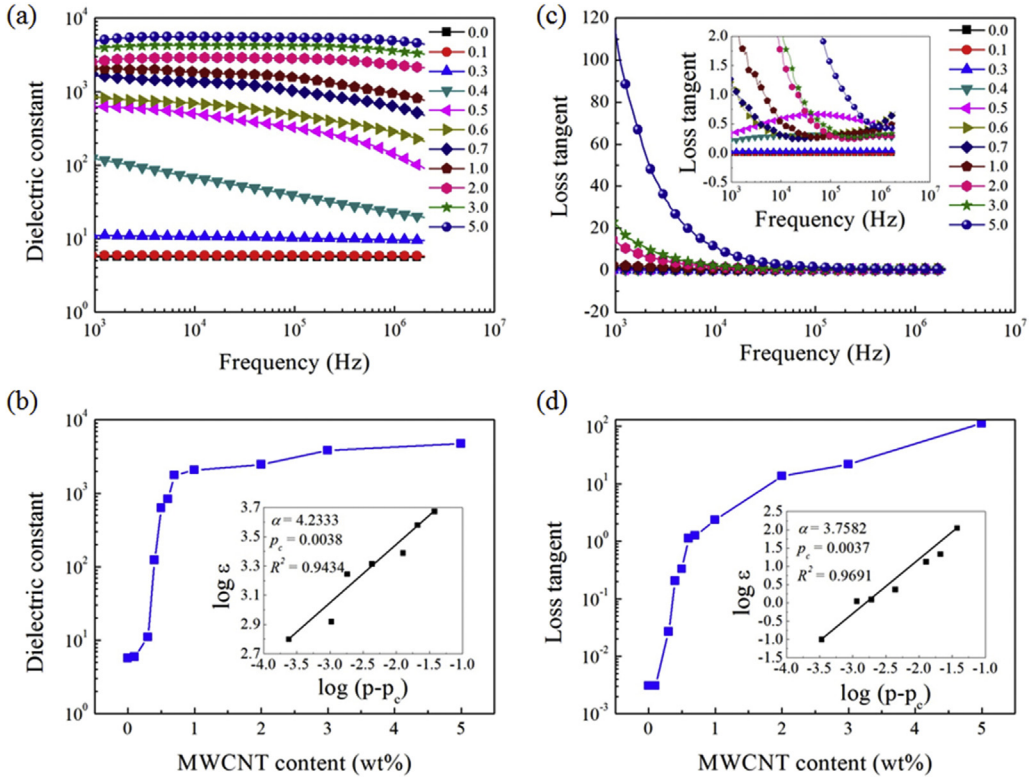

Fig. 4. (a) Dielectric constant-frequency curves and (b) dielectric constant at 1 kHz of PNGs with 30 wt% $BaTiO_3$ nanofiber and different MWCNT contents (0.0–5.0 wt%); (c) loss tangent-frequency curves and (d) loss tangent at 1 kHz of PNGs with 30 wt% $BaTiO_3$ nanofiber and different MWCNT contents (0.0–5.0 wt%). Insets in (b) and (d) are log ε *vs.* log (p-p_c) plot from the power law relation with the experimental dielectric data.

increase of frequency for the PNGs with MWCNT contents above 0.5 wt%. The loss tangent increased largely for the PNGs with high MWCNT contents above the critical content, which is attributed to the increase of current leakage current owing to high electrical conductivity. The percolation behavior of dielectric property was also evaluated by the power law relation $\varepsilon \sim (p\text{-}p_c)^{\alpha}$, in which ε is considered to be dielectric constant or loss tangent. The calculated critical MWCNT content for the percolation was ~0.38 vol% (~0.47 wt%) for dielectric constant and ~0.37 vol% (~0.46 wt%) for loss tangent, which are very consistent with the critical values estimated from the electrical conductivity data. The dielectric constant of PDMS/$BaTiO_3$(30)/MWCNT(0.0) was measured to be ~5.67, which is between neat PDMS (3.85) and $BaTiO_3$ nanofiber (100–11000). In case of PDMS/$BaTiO_3$(30)/MWCNT(5.0), a much higher dielectric constant of 4744.8 at 1 kHz was achieved, but also a large loss tangent of 113 was attained due to the leakage caused by higher contents of MWCNT with high conductivity. It is thus highly conjectured that the PNGs with <3.0 wt% MWCNTs, which possess high dielectric constants and low loss tangent values, can be used for high charge-storage capacitors and electrostriction system applications [23].

The output voltage and current of PDMS/$BaTiO_3$(30)/MWCNT(0.0–5.0) generated under a periodic mechanical pressure of 2 kPa are displayed in Fig. 5(a) and (b), respectively. When a mechanical pressure is applied to the PNGs, the piezoelectric potential generated by $BaTiO_3$ nanofibers leads charges to flow through an external circuit between top and bottom electrodes, which presents to be a negative peak. Subsequently, when the pressure is released, the charges flow back to the opposite direction, which presents to be a positive peak [1,26]. The output signals for PNGs with >1.0 wt% MWCNTs in the negative direction are found to be higher than the corresponding signals in the positive direction, because PNGs with high dielectric constants also act as capacitors. When a piezoelectric voltage is generated, induced charges are stored on the surface of the electrodes attached on PNGs. These stored charges will be consumed if an opposite voltage is applied. Therefore, the positive output voltages are smaller than the negative voltages [27]. The influence of high dielectric constants of the PNGs on the piezoelectric properties is also detected by the decay speed of positive voltage values. The decay speeds for the PNGs with 2.0–5.0 wt% MWCNTs are obviously slower than the those of the PNGs with 0.0–1.0 wt% MWCNTs, because the discharging speed is lower for the capacitor with higher capacitance or dielectric constant. All the average output voltage and current of the PNGs both in positive and negative directions are listed in Table 1. Based on the negative signals, the output voltage and current of PDMS/$BaTiO_3$(30)/MWCNT(0.0) are evaluated to be ~0.58 V and ~0.06 μA, respectively. The output values are 0.94 V and 0.15 μA for PDMS/$BaTiO_3$(30)/MWCNT(1.0) where MWCNT network is formed stably, as reflected from the frequency-dependent conductivity data. The PDMS/$BaTiO_3$(30)/MWCNT(2.0) generates a relative high output voltage of ~3.00 V and current of ~0.82 μA. The improved piezoelectric performance by incorporating MWNCT can be caused by various reasons. First, MWCNT with high modulus can enhance the stress transfer from flexible PDMS to nanofibers [2,28]. Second, the charge transfer between $BaTiO_3$ nanofibers can be improved by the existence of MWCNTs as electric bridges [13]. Third, mobile charges within MWCNT can facilitate the polarization of the PNGs, which also contributes to improve the piezoelectric property [29,30]. In cases of the PNGs with >2.0 wt% MWCNTs, the piezoelectric properties deteriorated seriously. Especially, PDMS/$BaTiO_3$(30)/MWCNT(5.0) produces a quite low output voltage of

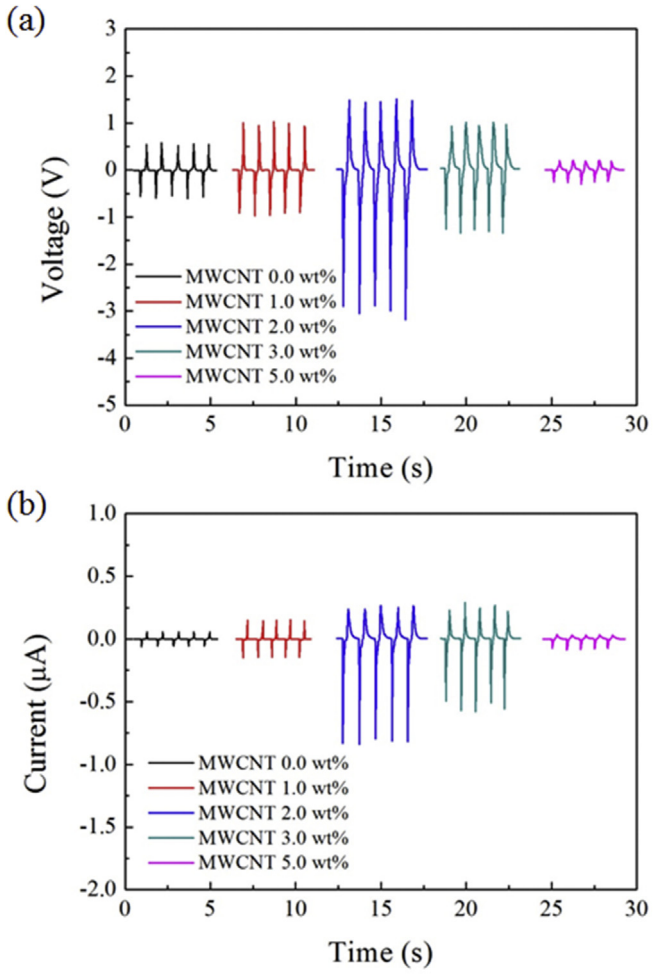

Fig. 5. (a) Output voltage and (b) current of PNGs with 30 wt% $BaTiO_3$ nanofiber and different MWCNT contents (0.0–5.0 wt%) under a periodic mechanical compression of 2 kPa.

~0.27 V and current of ~0.08 μA, which is even lower than PDMS/$BaTiO_3$(30)/MWCNT(0.0). This result is associated with the current leakage caused by exorbitant MWCNT among $BaTiO_3$ nanofibers in the PDMS matrix. The output power (P) of the PNGs subjected to the mechanical compression could be estimated from the following equation [31]:

$$P = \frac{1}{T}\int \frac{U^2(t)}{R}dt \quad (1)$$

where $U^2(t)$ is the square of the real-time voltage on the external load, R is the impedance of the external load (10 MΩ), T is the period of pressing and releasing. From the above equation, the average output powers of the PNGs are calculated and the results are summarized in Table 1. When the piezoelectric performance of the PNGs was plotted as a function of the MWCNT contents, as displayed in Fig. 6, it was found that the addition of 2.0 wt% MWCNT in the PNGs with constant 30 wt% $BaTiO_3$ nanofiber made the most significant improvement in the piezoelectric performance. PDMS/$BaTiO_3$(30)/MWCNT(2.0) generates a relative high output power of ~0.14 μW.

3.3. Role of $BaTiO_3$ nanofiber on structures and properties of PNGs

The PNGs with 10–50 wt% $BaTiO_3$ nanofibers and 2.0 wt%

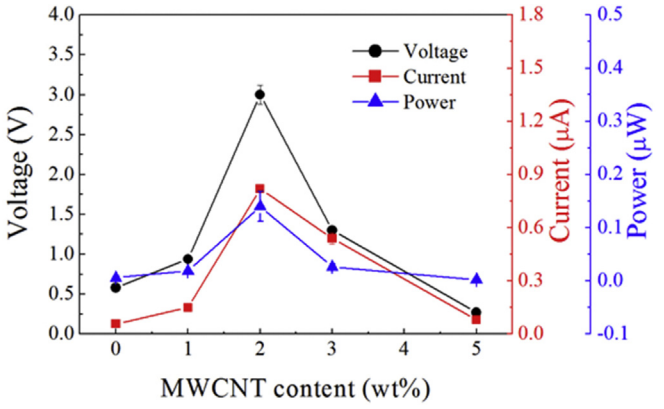

Fig. 6. Output voltage, current, and power of PNGs with 30 wt% $BaTiO_3$ nanofiber and different MWCNT contents (0.0–5.0 wt%) generated by a periodic mechanical compression of 2 kPa.

MWCNT were manufactured, and their electrical, dielectric, and piezoelectric properties were characterized as a function of the $BaTiO_3$ nanofiber content. To identify the dispersion state of $BaTiO_3$ nanofibers and MWCNTs, cross-sectional SEM images of the PNGs were obtained, as shown in Fig. 7, which exhibits that $BaTiO_3$ nanofibers and MWCNTs are uniformly dispersed in the PDMS matrix, except for the PNG with 50 wt% $BaTiO_3$ nanofibers.

The frequency-dependent AC conductivity and dielectric constant of the PNGs are illustrated in Fig. 8. It was found that both AC conductivity and dielectric constant of the PNGs with constant 2.0 wt% MWCNT increased with the increment of the $BaTiO_3$ nanofiber content. For all the PNGs, the AC conductivity remained unchanged at a low frequency range and increased significantly above a critical frequency, which is also higher for the PNGs with higher $BaTiO_3$ nanofiber contents. Both MWCNT and $BaTiO_3$ nanofiber play crucial roles in the increase of dielectric constants because they serve as microcapacitors in the PDMS matrix. The resulting AC conductivity and dielectric constant for the PNGs are listed in Table 1, which illustrates that the MWNCT content influences more significantly on dielectric properties, compared to the $BaTiO_3$ nanofiber content. The piezoelectric properties of the PNGs with different $BaTiO_3$ nanofiber contents were examined and the output signals are shown in Fig. 9. The output voltage and current increased to ~3.73 V and ~1.37 μA with increasing the $BaTiO_3$ nanofiber content up to 40 wt%, but they drop to a low value for the PNG with 50 wt% $BaTiO_3$ nanofiber because of the high current leakage due to its high conductivity as well as the nonuniform dispersion of $BaTiO_3$ nanofibers. The output powers of the PNGs were also calculated by Eq (1) and the results are listed in Table 1. When the piezoelectric performance of the PNGs with different $BaTiO_3$ nanofiber contents is displayed in Fig. 10, it was found that PNG with 40 wt% $BaTiO_3$ nanofiber has the highest outputs of ~3.73 V, ~1.37 mA, and ~0.33 μW.

It is believed that the superior performance of the PNGs attributes to the synergistic effect of $BaTiO_3$ nanofiber and MWCNT dispersed uniformly in the flexible PDMS matrix. In addition, a switching-polarity test was performed to verify the effectiveness of the output signals. Fig. 11 manifests the piezoelectric output signals of PDMS/$BaTiO_3$(40)/MWCNT(2.0) connected in the forward and reverse directions. When the electrodes of the samples were connected in the reverse direction, opposite voltage and current values were measured, which confirms that the output piezoelectric energy was purely generated from the PNGs triggered by a mechanical

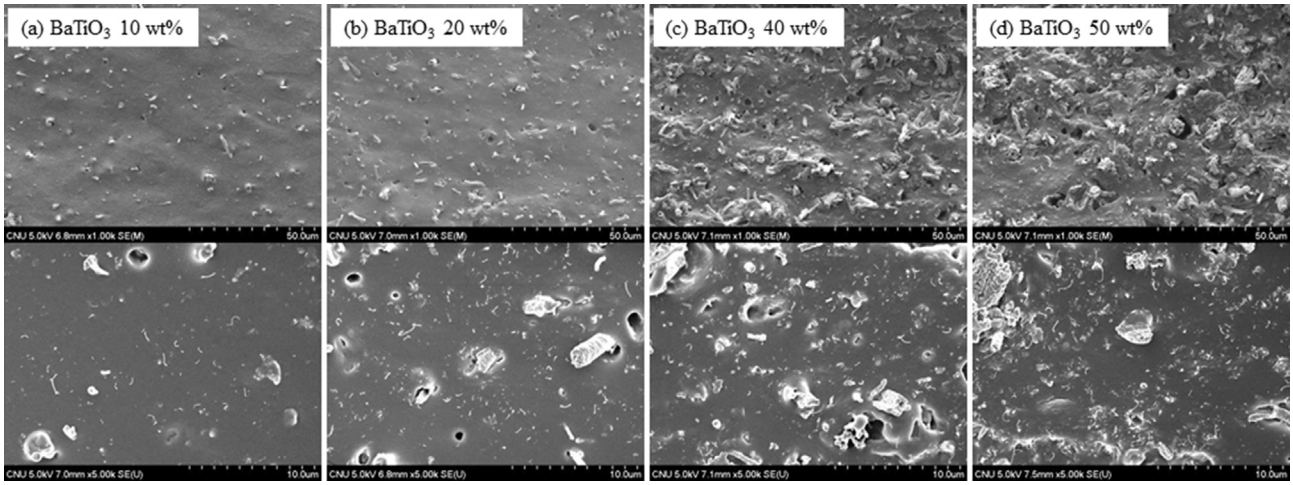

Fig. 7. Cross-sectional SEM images of PNGs with 2.0 wt% MWCNT and different $BaTiO_3$ nanofiber contents (10–50 wt%).

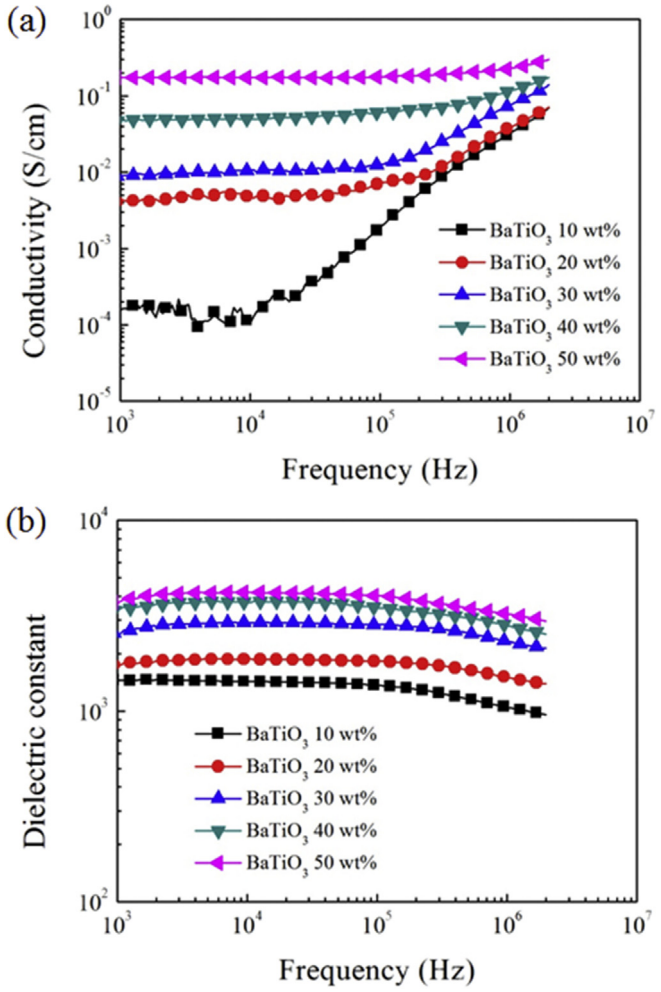

Fig. 8. (a) Conductivity and (b) dielectric constant of PNGs with 2.0 wt% MWCNT and different $BaTiO_3$ nanofiber contents (10–50 wt%).

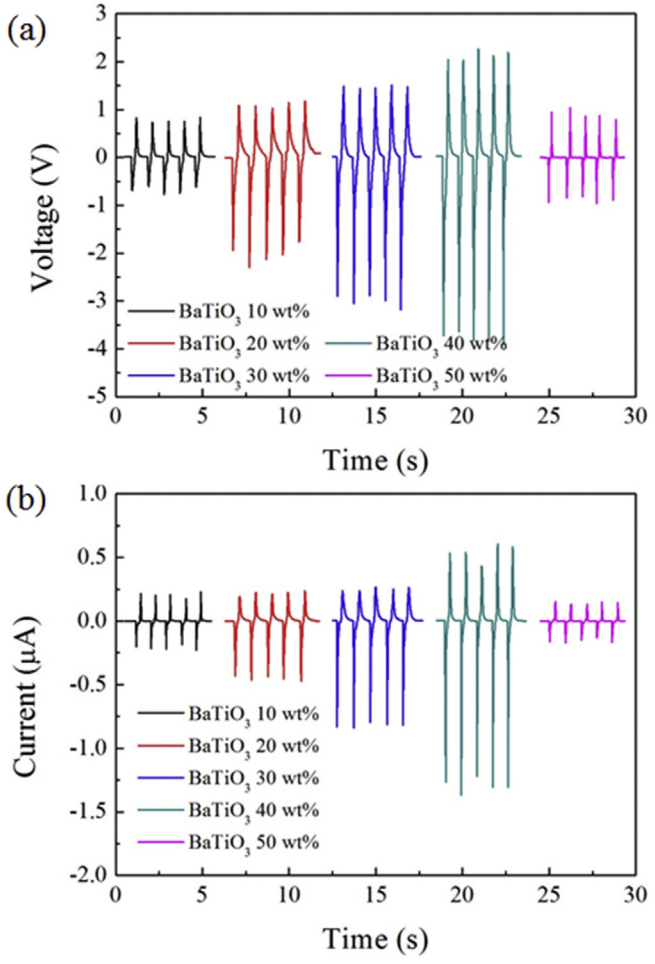

Fig. 9. (a) Output voltage and (b) current of PNGs with 2.0 wt% MWCNT and different $BaTiO_3$ nanofiber contents (10–50 wt%) under a periodic mechanical compression of 2 kPa.

pressure. The potential applications of PDMS/$BaTiO_3$(40)/MWCNT(2.0) were testified by lighting up commercial light-emitting diodes (LEDs) and charging capacitors. The generated electricity by the PNG was found to be high enough to light up one or two commercial LEDs instantly, although the light intensity was lower for two LEDs, as shown in a digital photographic image of

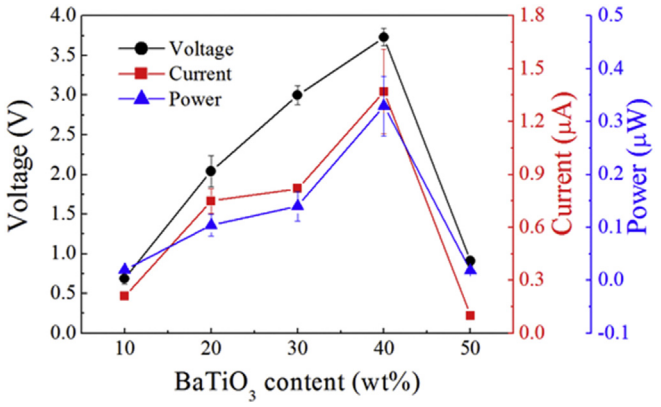

Fig. 10. Output voltage, current, and power of PNGs with 2.0 wt% MWCNT and different $BaTiO_3$ nanofiber contents (10–50 wt%) generated under a periodic mechanical compression of 2 kPa.

Fig. 12(a). To convert the produced AC output to DC signals, a full-wave bridge rectification circuit was used, as schematically depicted in Fig. 12(a). The rectified voltage and current shown in Fig. 12(b) and (c) are lower than the AC signals, which may be owing to the consumption by the rectifying diodes and/or a leakage of the capacitors [32]. The rectified piezoelectric energy of the PNGs scavenged from a periodically applied mechanical pressure was also high enough to charge up capacitors. The resulting time-dependent voltage charging processes are plotted in Fig. 12(d). The charged voltage increased exponentially with time to a steady state value of 0.8 V within 25 s for charging a 1.0 μF capacitor (with a rated voltage of 50 V), while 55 s was taken for charging 3.3 μF capacitors to the same voltage. The stepwise increases of the time-voltage curves support the effective energy conversion from mechanically applied pressure to electricity, as represented in the inset of Fig. 12(d) where the pink and green arrowheads indicate the pressing and releasing of a periodic mechanical compression, respectively.

4. Conclusions

In summary, the roles and contents of MWCNT (0.0–5.0 wt%) and $BaTiO_3$ nanofiber (10–50 wt%) in the electrical, dielectric and piezoelectric properties of PDMS-based PNGs were systematically investigated. SEM images revealed that MWCNT and $BaTiO_3$ nanofibers were effectively dispersed in the PDMS matrix of the flexible PNGs manufactured with the assistance of ultrasonication and ethyl acetate solvent. Firstly, when the influences of MWCNT (0.0–5.0 wt%) in the PNGs with constant 30 wt% $BaTiO_3$ nanofiber on the electrical and dielectric properties were investigated, it was revealed that the percolation behaviors were observed at the critical MWCNT content of ~0.38 vol% (0.47 wt%) and that the PNG with 2.0 wt% MWCNT exhibited a high piezoelectric performance of output voltage of ~3.00 V, current of ~0.82 μA, and power of ~0.14 μW under a periodic mechanical compression of 2 kPa. Secondly, when the effects of $BaTiO_3$ nanofiber (10–50 wt%) on the properties of PNGs with constant 2.0 wt% MWCNT were evaluated, it was found that the conductivity and dielectric constant increased with the increment of $BaTiO_3$ nanofiber content and that the PNG with 40 wt% $BaTiO_3$ nanofiber possessed the best piezoelectric performance of output voltage of ~3.73 V, current of ~1.37 μA, and power of ~0.33 μW. The piezoelectric power generated by a periodic pressing-releasing process was found to be feasible to light up commercial LEDs and to charge a capacitor after rectification. Overall, it is valid to contend that the PNG system based on PDMS, $BaTiO_3$ nanofiber and MWCNT can be used as an energy harvester for powering self-sufficient nanodevices and wireless electronics.

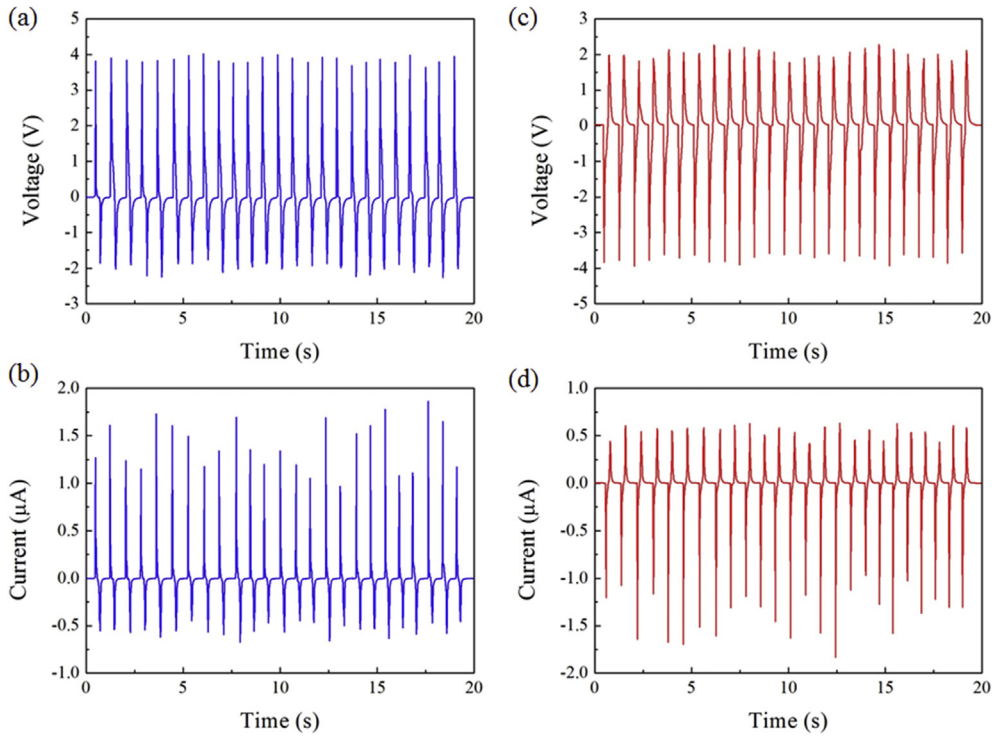

Fig. 11. Output voltage and current of PDMS/$BaTiO_3$(40)/MWCNT(2.0) in (a, b) forward direction and (c, d) reverse direction under a periodic mechanical compression of 2 kPa.

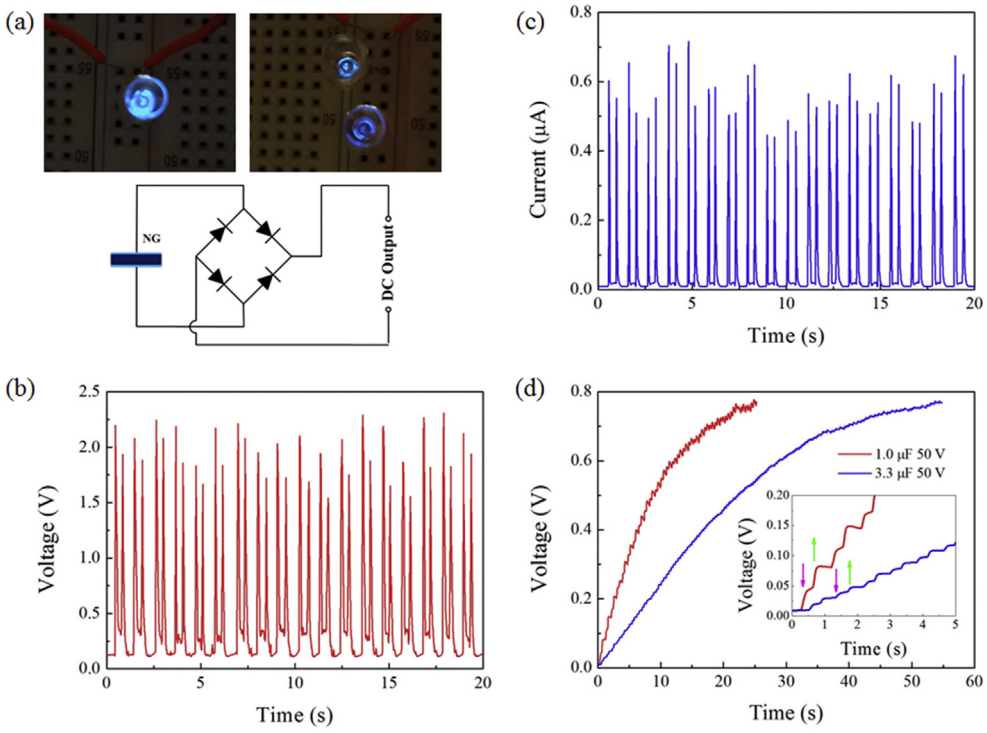

Fig. 12. (a) Digital photographic images of one and two commercial blue LEDs lit up by the electric energy generated by PDMS/$BaTiO_3$(40)/MWCNT(2.0) and a schematic circuit diagram for rectifying; (b) voltage and (c) current signals after the rectification; (d) time-dependent voltage charging curves of capacitors with different capacitances. Pink and green arrowheads in inset of (d) indicate the pressing and releasing of mechanical compression, respectively. (For interpretation of the references to colour in this figure legend, the reader is referred to the web version of this article.)

Acknowledgements

This work was supported by the National Research Foundation of Korea (NRF) Grant funded by the Korean Government (MOE) (2016R1D1A1B03932942).

References

[1] Z.-H. Lin, Y. Yang, J.M. Wu, Y. Liu, F. Zhang, Z.L. Wang, $BaTiO_3$ nanotubes-based flexible and transparent nanogenerators, J. Phys. Chem. Lett. 3 (23) (2012) 3599–3604.
[2] K.I. Park, M. Lee, Y. Liu, S. Moon, G.T. Hwang, G. Zhu, et al., Flexible nanocomposite generator made of $BaTiO_3$ nanoparticles and graphitic carbons, Adv. Mater. 24 (22) (2012) 2999–3004.
[3] G.H. Kim, S.M. Hong, Y. Seo, Piezoelectric properties of poly(vinylidene fluoride) and carbon nanotube blends: b-phase development, Phys. Chem. Chem. Phys. 11 (44) (2009) 10506–10512.
[4] C.J. Hu, Y.H. Lin, C.W. Tang, M.Y. Tsai, W.K. Hsu, H.F. Kuo, ZnO-coated carbon nanotubes: flexible piezoelectric generators, Adv. Mater. 23 (26) (2011) 2941–2945.
[5] K.I. Park, J.H. Son, G.T. Hwang, C.K. Jeong, J. Ryu, M. Koo, et al., Highly-efficient, flexible piezoelectric PZT thin film nanogenerator on plastic substrates, Adv. Mater. 26 (16) (2014) 2514–2520.
[6] Y. Wei, Y. Song, X. Deng, B. Han, X. Zhang, Y. Shen, et al., Dielectric and ferroelectric properties of $BaTiO_3$ nanofibers prepared via electrospinning, J. Mater Sci. Technol. 30 (8) (2014) 743–747.
[7] V. Petrovsky, T. Petrovsky, S. Kamlapurkar, F. Dogan, Dielectric constant of barium titanate powders near Curie temperature, J. Am. Ceram. Soc. 91 (11) (2008) 3590–3592.
[8] M.T. Buscaglia, M. Viviani, V. Buscaglia, L. Mitoseriu, A. Testino, P. Nanni, et al., High dielectric constant and frozen macroscopic polarization in dense nanocrystalline $BaTiO_3$ ceramics, Phys. Rev. B 73 (6) (2006) 064114.
[9] M.M. Vijatović, J.D. Bobić, B.D. Stojanović, History and challenges of barium titanate: Part II, Sci. Sinter. 40 (3) (2008) 235–244.
[10] B. Ertuğ, The overview of the electrical properties of barium titanate, Am. J. Eng. Res. 2 (8) (2013) 1–7.
[11] S.H. Lee, D.H. Lee, W.J. Lee, S.O. Kim, Taiored assembled of carbon nanotubes and graphene, Adv. Funct. Mater. 21 (8) (2011) 1338–1354.
[12] D.S. Tucker, X. Wang, K. Stano, P.D. Bradford, M. Allen, M. Sanghadasa, et al., Robust aligned carbon nanotube tape with excellent piezoelectric properties, Recent Prog. Space Technol. 4 (2) (2014) 110–118.
[13] H. Sun, H. Tian, Y. Yang, D. Xie, Y.-C. Zhang, X. Liu, et al., A novel flexible nanogenerator made of ZnO nanoparticles and multiwall carbon nanotube, Nanoscale 5 (13) (2013) 6117–6123.
[14] Y. Ahn, J.Y. Lim, S.M. Hong, J. Lee, J. Ha, H.J. Choi, et al., Enhanced piezoelectric properties of electrospun poly(vinylidene fluoride)/multiwalled carbon nanotube composites due to high β-phase formation in poly(vinylidene fluoride), J. Phys. Chem. C 117 (22) (2013) 11791–11799.
[15] Y. Hao, H. Tao, L. Mingxia, M. Mengye, Z. Qinghong, W. Hongzhi, Enhanced power output of an electrospun PVDF/MWCNTs-based nanogenerator by tuning its conductivity, Nanotechnology 24 (40) (2013) 405401.
[16] S.K. Mahadeva, K. Walus, B. Stoeber, Piezoelectric paper fabricated via nanostructured barium titanate functionalization of wood cellulose fibers, ACS Appl. Mater. Interfaces 6 (10) (2014) 7547–7553.
[17] S.D. Vacche, F. Oliveira, Y. Leterrier, V. Michaud, D. Damjanovic, J.-A.E. Månson, The effect of processing conditions on the morphology, thermomechanical, dielectric, and piezoelectric properties of P (VDF-TrFE)/BaTiO3 composites, J. Mater. Sci. 47 (11) (2012) 4763–4774.
[18] J. Yan, Y.G. Jeong, High performance flexible piezoelectric nanogenerators based on $BaTiO_3$ nanofibers in different alignment modes, ACS Appl. Mater. Interfaces 8 (24) (2016) 15700–15709.
[19] H.B. Kang, J. Chang, K. Koh, L. Lin, Y.S. Cho, High quality Mn-doped (Na,K)NbO_3 nanofibers for flexible piezoelectric nanogenerators, ACS Appl. Mater. Interfaces 6 (13) (2014) 10576–10582.
[20] J. Yan, Y.G. Jeong, Multiwalled carbon nanotube/polydimethylsiloxane composite films as high performance flexible electric heating elements, Appl. Phys. Lett. 105 (5) (2014) 051907.
[21] S. Barrau, P. Demont, A. Peigney, C. Laurent, C. Lacabanne, DC and AC conductivity of carbon nanotubes-polyepoxy composites, Macromolecules 36 (14) (2003) 5187–5194.
[22] A.K. Jonscher, The 'universal' dielectric response, Nature 267 (1977) 673–679.
[23] Q. Li, Q. Xue, Q. Zheng, L. Hao, X. Gao, Large dielectric constant of the chemically purified carbon nanotube/polymer composites, Mater. Lett. 62 (26) (2008) 4229–4231.
[24] S.-H. Yao, Z.-M. Dang, M.-J. Jiang, J. Bai, $BaTiO_3$-carbon nanotube/polyvinylidene fluoride three-phase composites with high dielectric constant and low dielectric loss, Appl. Phys. Lett. 93 (18) (2008) 182905.
[25] L. Seveyrat, A. Chalkha, D. Guyomar, L. Lebrun, Preparation of graphene nanoflakes/polymer composites and their performances for actuation and energy harvesting applications, J. Appl. Phys. 111 (10) (2012) 104904.
[26] S.-H. Shin, Y.-H. Kim, M.H. Lee, J.-Y. Jung, J. Nah, Hemispherically aggregated $BaTiO_3$ nanoparticle composite thin film for high-performance flexible

piezoelectric nanogenerator, ACS Nano 8 (3) (2014) 2766–2773.
[27] S. Xu, Y. Yeh, G. Poirier, M.C. McAlpine, R.A. Register, N. Yao, Flexible piezoelectric PMN–PT nanowire-based nanocomposite and device, Nano Lett. 13 (6) (2013) 2393–2398.
[28] W.R. McCall, K. Kim, C. Heath, G. La Pierre, D.J. Sirbuly, Piezoelectric nanoparticle-polymer composite foams, ACS Appl. Mater. Interfaces 6 (22) (2014) 19504–19509.
[29] J. Kim, K.J. Loh, J.P. Lynch, Piezoelectric polymeric thin films tuned by carbon nanotube fillers, in: M. Tomizuka (Ed.), Sensors and Smart Structures Technologies for Civil, Mechanical, and Aerospace Systems 2008, International Society for Optics and Photonics, 2008, p. 693232.
[30] I.-H. Kim, D.H. Baik, Y.G. Jeong, Structures, electrical, and dielectric properties of PVDF-based nanocomposite films reinforced with neat multi-walled carbon nanotube, Macromol. Res. 20 (9) (2012) 920–927.
[31] T. Gao, J. Liao, J. Wang, Y. Qiu, Q. Yang, M.Q. Zhang, et al., Highly oriented $BaTiO_3$ film self-assembled using an interfacial strategy and its application as a flexible piezoelectric generator for wind energy harvesting, J. Mater. Chem. A 3 (18) (2015) 9965–9971.
[32] S. Xu, B.J. Hansen, Z.L. Wang, Piezoelectric-nanowire-enabled power source for driving wireless microelectronics, Nat. Commun. 1 (2010) 93.